Journal of Mammalogy, 95(1):E1–E15, 2014

Integrative taxonomy within the *Hylomyscus denniae* complex (Rodentia: Muridae) and a new species from Kenya

Terrence C. Demos,* Bernard Agwanda, and Michael J. Hickerson

Biology Department, The City College of New York, 160 Convent Avenue, New York, NY 10031, USA (TCD, MJH)
Biology Doctoral Program, The Graduate Center, City University of New York, 365 5th Avenue, New York, NY 10016, USA (TCD, MJH)
Department of Zoology, Field Museum of Natural History, 1400 South Lake Shore Drive, Chicago, IL 60605, USA (TCD)
Mammalogy Section, National Museums of Kenya, P.O. Box 40658, Nairobi, Kenya (BA)

* *Correspondent: terrencedemos@gmail.com*

A new species of African wood mouse (*Hylomyscus*) is described from the western Kenya region. Previous studies have hypothesized that populations of *Hylomyscus* from this region may be assignable to either *H. vulcanorum* or *H.* cf. *anselli*. We compared 3 populations of *Hylomyscus* from western Kenyan montane forests to sister taxa from the *Hylomyscus denniae* group on the basis of morphology, morphometrics, mitochondrial DNA gene trees, multilocus species trees, and coalescent-based species delimitation to clarify relationships within these clades. Our results were congruent across data sets in support of this new species as sister to *H. anselli* and reproductively isolated from *H. endorobae* on the Mau Escarpment of Kenya where the 2 taxa are sympatric and syntopic. Lineages within the *H. anselli* group differ by 3.2–7.4% in (corrected) cytochrome-*b* sequences. Phylogeographic analysis of *Hylomyscus* n. sp. suggests strong population or range expansion, or both, since the last glacial maxima. A dated multilocus species tree places divergence of *Hylomyscus* n. sp. from *H. anselli* during the middle Pleistocene and the *H. anselli* group from the *H. denniae* group during the late Miocene to early Pliocene. This species is known from protected sites on Mt. Elgon, as well as unprotected sites within the Mau Escarpment and Cherangani Hills where extensive human habitat disturbance warrants conservation attention.

Key words: Afromontane, cryptic species, *Hylomyscus*, Kenya, Muridae, phylogeography, species tree

DOI: 10.1644/13-MAMM-A-268

The woodland mice of the genus *Hylomyscus* Thomas, 1926, are members of the diverse tribe Praomyini, an African lineage that is estimated to have originated 7.6 million years ago (mya; ± 0.5 mya—Lecompte et al. 2008). These are small-sized rodents that are geographically restricted to forests of tropical Africa where they are often an abundant component of the rodent fauna (Kerbis Peterhans et al. 1998; Nicolas and Colyn 2003; Stanley and Hutterer 2007). On the basis of external and cranial morphology *Hylomyscus* species have been assigned to 6 species groups: *aeta*, *alleni*, *anselli*, *baeri*, *denniae*, and *parvus* (Carleton et al. 2006). Recently, species assignment within these groups has been subject to substantial revision because of the cryptic nature of morphological diversity within species groups, the disjunct and patchy distribution of populations of *Hylomyscus*, and lack of adequate comparative series of specimens for some taxa. Two montane forest–restricted species groups distributed across south-central and eastern Africa, the *Hylomyscus denniae* and *Hylomyscus anselli* groups, have recently been revised on the basis of morphological characters and multivariate morphometric analyses (Carleton and Stanley 2005; Carleton et al. 2006). These revisions assigned 3 and 2 species to each of the aforementioned groups, respectively. Within the *H. anselli* group, members occur in mountains of northern Zambia and southwestern Tanzania (*H. anselli*; also see Bryja et al. 2012), across the Eastern Arc Mountains and Mount Rungwe of Tanzania (*H. arcimontensis*), and the central Angolan Highlands (*H.* aff. *anselli*). Members of the *H. denniae* group are documented from the Ruwenzori Mountains of western Uganda and eastern Democratic Republic of the Congo (*H. denniae*); a 2nd species (*H. vulcanorum*) is more widespread and extends from Tshiabirimu in the north to the Itombwe

Massif in the south, as well as the mountains of Burundi, Rwanda, and southwestern Uganda; whereas the 3rd species (*H. endorobae*) occurs in the highlands of west-central Kenya including Mt. Kenya, the Aberdare Mountains, and the Mau Escarpment.

Although Bishop (1979), in a subspecific revision of East African populations of *Hylomyscus* (i.e., which are currently recognized as members of the *Hylomyscus stella*, *H. denniae*, and *H. anselli* groups), noted affinities between specimens of *Hylomyscus* from the Cherangani Hills and Mt. Elgon with those from Zambia he had assigned to *Praomys* (*Hylomyscus*) *denniae anselli*, he nonetheless provisionally assigned the western Kenyan specimens to *Praomys* (*Hylomyscus*) *denniae vulcanorum*. He noted similarities in occipitonasal length and crown length of upper molar row between populations from Zambia and those from the Cherangani Hills and Mt. Elgon. Carleton et al. (2006) in their review of the *H. denniae* group noted that the few specimens of *Hylomyscus* from the eastern slopes of Mt. Elgon examined were examples of the *H. anselli* complex, not the *H. denniae* complex, as attributed to specimens from the Ugandan slopes of Mt. Elgon by Clausnitzer and Kityo (2001). In addition, Carleton et al. (2006) reported examples of *H.* cf. *anselli* from the Guas Ngishu Plateau and the Mau Escarpment, both in west-central Kenya. They note that clarification of species identifications of Mt. Elgon specimens is the subject of unpublished research and that *H.* cf. *anselli* from western Kenya may prove to be sympatric with *H. endorobae*. Carleton et al. (2006) note that specimens found within 4 miles (6.4 km) of one another on the Mau Escarpment are referable to both *H. endorobae* and *H.* cf. *anselli*, thus possibly sympatric elsewhere. They call for additional collecting to clarify the taxonomic status of Kenyan *Hylomyscus*, in particular those populations from montane forests west of the Gregory Rift where they provisionally assign specimens to *H.* cf. *anselli* but defer from ascribing species status. However, Carleton et al. (2006) include no measurements or qualitative characters for any of the specimens they provisionally assign to the *H. anselli* group.

It has been proposed that the description of species presenting taxonomic uncertainties, particularly in relation to cryptic taxa, should integrate independent lines of evidence such as morphological, molecular, geographical, and ecological data (Fujita et al. 2012). The incorporation of coalescent-based methods into phylogenetic and population genetic analyses that allow for uncertainty in gene trees and account for incomplete lineage sorting due to ancestral polymorphisms provide powerful tools for inferring evolutionary relationships among species and species delimitation (Riddle et al. 2008; Hickerson et al. 2010). Our objectives in this study are to apply multiple lines of evidence in an integrative taxonomic approach to characterize several populations of western Kenya montane forest *Hylomyscus* in relation to a large data set of specimens from throughout the geographic ranges of members of the *H. denniae* and *H. anselli* species complexes, in order to describe a new species from western Kenya (Fig. 1). We also document patterns of morphological and genetic variation that assist in discriminating between specimens of these 2 species groups that are currently known to be sympatric in the Mau Escarpment. Finally, we present phylogeographic and ecological data that shed light on the roles of Pleistocene forest refugia and niche conservatism in shaping the current distributions of Kenyan montane *Hylomyscus*.

Materials and Methods

Specimens of *Hylomyscus* were collected during small mammal surveys of the forests of the Kenyan Highlands with additional comparative material obtained from the Field Museum of Natural History (FMNH; Fig. 1). These surveys were conducted from 2010 to 2011 by associates and staff of FMNH and the National Museums of Kenya (NMK). Rodent specimens were captured using a combination of snap traps and Sherman live traps (H. B. Sherman Traps, Inc., Tallahassee, Florida) based on small mammal trapping protocols as previously implemented by J. Kerbis Peterhans and W. Stanley of FMNH (Kerbis Peterhans et al. 1998; Stanley et al. 1998). Specimens were measured and weighed, and either prepared as skins and skeletons or preserved in formalin and later stored in 70% ethanol, and deposited in FMNH and NMK. All the specimens examined in this study are listed in Appendix I, and their collecting localities are indicated in Fig. 1 and described in Appendix I. For animal care and use, we followed guidelines approved by the American Society of Mammalogists (Sikes et al. 2011).

Discrimination between species was based on craniodental morphology, multivariate morphometric analyses, species distribution models, and multilocus molecular data under a coalescent species-tree framework. Species designations were corroborated by multilocus DNA sequencing of 43 specimens (*Hylomyscus* n. sp., $n = 12$; *H. anselli*, $n = 3$; *H. arcimontensis*, $n = 3$; *H. denniae*, $n = 4$; *H. endorobae*, $n = 11$; *H. vulcanorum*, $n = 7$; and *H. stella*, $n = 3$) for inclusion in coalescent-based species tree, Bayesian species delimitation, and demographic analyses. We included *H. stella* to test for multilocus divergence from the *H. anselli* group because preliminary mitochondrial DNA (mtDNA) analyses supported this species as sister to *H. anselli*. These analyses were carried out using 3–5 autosomal nDNA introns: GAD2-1 and JMJD5-2 using primers that have been filtered as optimal for phylogenetics of closely related mammal species and designed to sequence across a wide spectrum of mammalian orders (Igea et al. 2010); ABHD11-5, ACOX2-3, and ACPT-4 (optimized for *Myotis* – Salicini et al. 2011); and mtDNA Cytochrome-*b* (*CytB* – Lecompte et al. 2002) sequence data. We selected intron primers based on prior testing for absence of paralogy, levels of variability, ease of amplification across Mammalia, and availability of published primer sequences (Igea et al. 2010; Salicini et al. 2011). A larger data set of *Cytb* sequence data was used to infer a gene tree based on 81 specimens (*Hylomyscus* n. sp., $n = 41$; *H. anselli*, $n = 5$; *H. arcimontensis*, $n = 8$; *H. endorobae*, $n = 25$; *H. vulcanorum*, $n = 2$; *H. denniae*, $n = 2$; *H. stella*, $n = 4$; *H. aeta*, $n = 1$; and 1 outgroup).

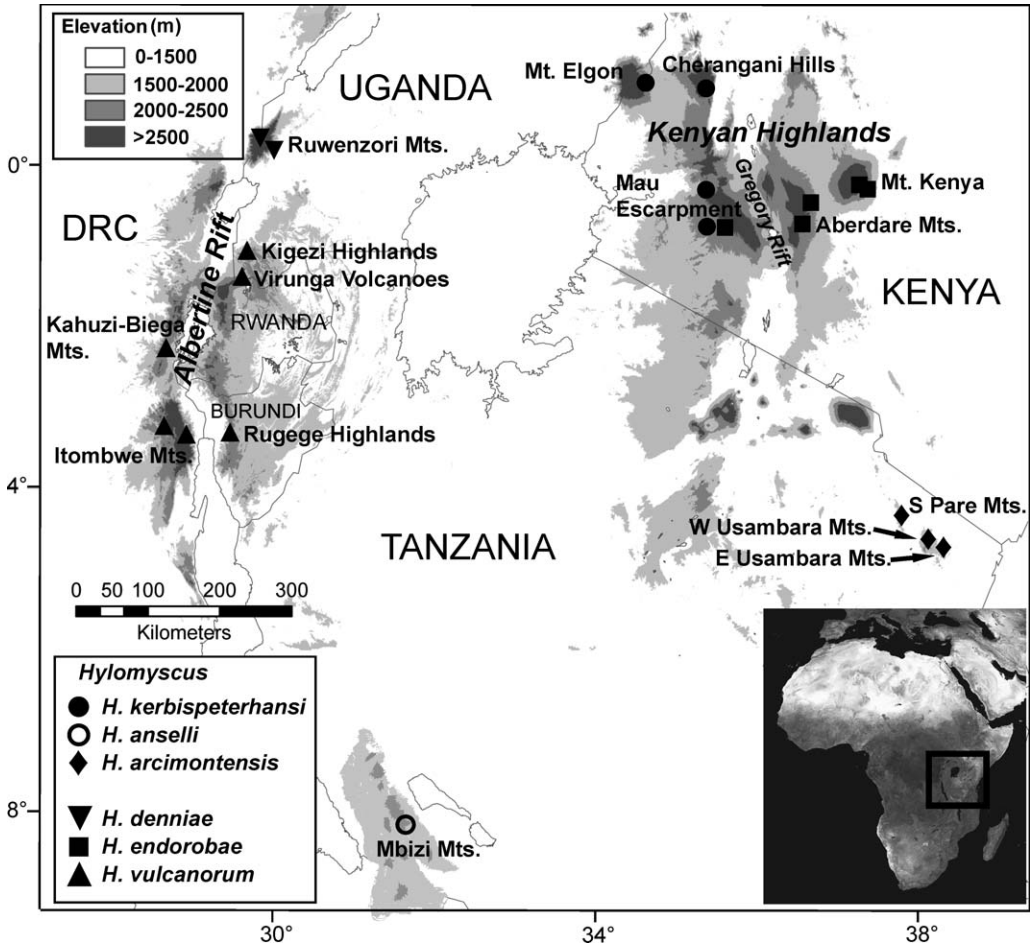

Fig. 1.—Map of the collecting localities for the specimens of *Hylomyscus* included in this study. Elevation indicated by gray shading as defined on map. See Appendix I for additional specimens examined for morphometric and molecular analyses.

Genomic DNA was extracted using the QIAgen DNeasy Blood and Tissue Kit (Qiagen Inc., Valencia, California). Polymerase chain reaction amplifications were performed in either 25- or 50-ml reactions using the following thermal conditions: an initial denaturing step at 94°C for 2 min; 35–39 cycles of denaturing at 94°C for 30 s, annealing varying in the range 50–62°C for 30 s, extension at 72°C for 60 s for introns and at 68°C for 68 s for *Cytb*, followed by a final extension step at 68°C for 5 min for introns and 72°C for 7 min for *Cytb*. Polymerase chain reaction products were purified using either spin columns in our laboratory or ExoSAP-IT at the sequencing facility. Sequencing was performed directly using the corresponding polymerase chain reaction primers. DNA sequences of both strands were obtained using the BigDye Terminator (Applied Biosystems, Carlsbad, California) on ABI DNA analyzers (Applied Biosystems) at Macrogen Inc. (Seoul, Korea) and University of Washington High Throughput Sequencing (Seattle, Washington).

Chromatographs were checked manually and assembled and edited using Geneious Pro 6.0.5 (Drummond et al. 2013). Sequences were aligned for each locus using MUSCLE Alignment within the Geneious platform under default parameters. Predicted amino acid sequences from *Cytb* sequences were inspected for deletions, insertions, and premature stop codons to exclude possible nuclear pseudogenes. Alignments for all data sets were unambiguous for all nuclear and mtDNA loci examined. Recombination was tested with the Detect Recombination plugin in Geneious. We used the PHASE 2.1 algorithm to statistically resolve haplotypes from the nuclear intron sequences (Smith et al. 2005; Stephens et al. 2001). Sequences were accessioned into GenBank (KF810147–KF810515 and KF876466–KF876548).

For the *Cytb* data set genetic variability was assessed using DnaSP version 5 (Librado and Rozas 2009) to calculate nucleotide diversity (π), haplotype diversity (H_d), and number of segregating sites (S) per taxon. Total and net divergence between species using Tamura–Nei distances was calculated in MEGA version 5.2 (Tamura et al. 2007). jModelTest version 2.1 (Guindon and Gascuel 2003; Darriba et al. 2012) was used to assign the most appropriate model of sequence evolution using the Akaike information criterion (AIC). We used MrBayes version 3.2 (Ronquist et al. 2012) to infer gene trees for *Cytb* and intron data independently. Gene-tree analyses involved 2 runs of 4 heated chains for 1×10^7 generations with 10% as burn-in and a sampling frequency that provided 5,000 samples for each run. Convergence of Bayesian Markov chain

Monte Carlo gene-tree analysis was assessed by examining likelihood and parameter estimates in Tracer version 1.5 (Rambaut and Drummond 2007) to confirm effective sample sizes of at least 200, indicating adequate sampling of posterior distributions.

To delimit isolated populations and infer species status among major population lineages, we used the approach of Leaché and Fujita (2010) implemented in Bayesian Phylogenetics and Phylogeography v2.1 (BPP; Yang and Rannala 2010) and described in detail in Demos et al. (2013). We treated collecting localities among mountain ranges as putative populations with allele samples, eliminating the need to carry out *a priori* population assignments on the basis of either inferred mtDNA gene trees or genotypic clustering algorithms that to assign alleles to putative populations. It has been shown (Yang and Rannala 2010; Leaché and Fujita 2010; Camargo et al. 2012) that designating localities as putative populations prior to the BPP delimitation is a conservative approach that consistently recovers the same genetically isolated populations.

The BPP reversible-jump Markov chain Monte Carlo analyses were run for 5×10^5 generations with a burn-in of 5,000 generations and repeated to ensure consistent results with different starting seeds. We did preliminary tests of species delimitation algorithms 0 and 1 and obtained very similar results with both; thus, algorithm 0 was used with fine-tuning parameter $\varepsilon = 5.0$. We estimated prior distributions for ancestral population size (θ) based on DNAsp ($\theta_W = 0.01$–0.028) and root age (τ_0) based on a dated phylogeny inferred in *BEAST (Drummond and Rambaut 2007; Drummond et al. 2012) assuming an nDNA mutation rate of $\sim 2 \times 10^{-8}$ mutations per site (Nachman and Crowell 2000) giving a gamma distribution of (θ) G(1, 10) and (τ_0) G(1, 33), with prior means = 0.01 and 0.03 and variances = 0.001 and 0.003, respectively. We consider speciation probability values >0.98 as strongly supporting a speciation event.

Species delimitation under BPP requires an inferred species tree that acts as a guide tree specifying initial relationships among populations in an analysis. This was accomplished using the coalescent-based species-tree approach implemented in *BEAST, an extension of BEAST v1.7.4 (Drummond et al. 2012; Drummond and Rambaut 2007). Species tree relationships within *Hylomyscus* were inferred using *Cytb* mtDNA and 3 nDNA intron sequences, with *Cytb* partitioned by codon (1, 2, and 3). Models of sequence evolution were estimated using the AIC criterion in TOPALi v2.5 (Milne et al. 2009). The input file for the guide tree for BPP was formatted using the BEAUti utility (Drummond et al. 2012). We generated 2 independent runs for 3×10^8 generations and sampled every 1,000 generations in BEAST.

In order to infer the relationship of lineage splitting times with Plio-Pleistocene climatic fluctuations, we used substitution rates from closely related taxa based on recent empirical studies that utilized fossil calibrations to estimate *Cytb* substitution rates. We used a *Cytb* rate of 0.025 substitutions site^{-1} Myr^{-1} estimated for the sister genus *Praomys* based on 2 African murid fossil dates (Nicolas et al. 2011). We acknowledge that these calibrations will likely be upwardly biased in coalescent-based species tree applications because these previous studies ignore gene-tree/species-tree discordance (Edwards and Beerli 2000), and as such are relatively crude estimates of divergence dates.

Convergence of model parameters for *BEAST analyses was assessed based on ESS values and examination of trace files using Tracer v1.5 (Rambaut and Drummond 2007). The initial 10% of each run were discarded as burn-in and separate runs were combined using LogCombiner. The maximum clade credibility tree was generated in TreeAnnotator.

Historical population size changes were inferred for Kenyan populations of *H. endorobae* and *H.* cf. *anselli* using the coalescent-based extended Bayesian skyline plot (EBSP) implemented in *BEAST for combined mtDNA and nDNA data. The same substitution rates that were used in the species tree analyses were used as reference rates for *Cytb* and intron rates were scaled to these. Substitution models for all loci were estimated in TOPALi. Sequences from *Cytb* and 5 nDNA loci per lineage were included in a given population analysis using an uncorrelated lognormal relaxed-clock. The input file for the analyses was generated in BEAUTi using both EBSP author suggestions for prior settings and default settings, and 2 replicate runs of 1.5×10^8 generations were run.

Five external measurements (in mm) were transcribed from field notes as recorded by collectors that included total length (TOT), tail length (TAIL), head and body length (HB; calculated by subtracting TAIL from TOT), hind-foot length with claw (HF), and ear length (EAR); and body mass (WT, in g). Fourteen cranial and dental variables following Carleton and Stanley (2005) were measured using digital calipers (Mitutoyo, Kawasaki, Japan) to the nearest 0.01 mm while examining crania under a dissecting microscope. The measurements taken were: occipitonasal length (ONL); greatest zygomatic breadth (ZB); breadth of braincase (BBC), measured across the parietal flanges behind the zygomatic arches; breadth across occipital condyles (BOC); least interorbital breadth (LOB); breadth of rostrum (BR); postpalatal length (PPL); length of bony palate (LBP); length of incisive foramen (LIF); length of diastema (LD); breadth of zygomatic plate (BZP); length of auditory bulla (LAB); crown length of upper molariform toothrow (CLM); and greatest width of 1st upper molar from lingual to buccal surfaces (WM1). Multivariate analyses were restricted to these 14 skull characters, because external measurements in the field are known to be highly variable depending on the collector taking the measurements. We include external measurements by the senior author (*H.* cf. *anselli* and *H. endorobae*) and W. T. Stanley (*H. anselli* and *H. arcimontensis*—Carleton and Stanley 2005) for use in univariate statistical comparisons only.

Only specimens that were determined to be adult on the basis of worn fully erupted 3rd molars and adult pelage were used for morphometric analyses. Sexual dimorphism in cranial and dental morphometric variables has been evaluated previously within *Hylomyscus* and was not found to be significant (Carleton and Stanley 2005; Nicolas et al. 2008),

and therefore we combined the sexes for morphometric analyses.

Discriminant analysis and ordination of canonical variates were used to assess morphometric differences between species. Statistically significant differences between designated species group centroids were evaluated by means of Mahalanobis distances and Wilks' lambda statistics. All multivariate analyses were based on log-transformed craniodental morphometric data. Additional analyses included standard univariate descriptive statistics. All statistical analyses were performed using algorithms in R (R Development Core Team 2013) and STATISTICA version 10 (StatSoft Inc. 2011).

Results

On the basis of the morphological and molecular phylogenetic characters described in the following sections, we recognize specimens of *Hylomyscus* from the Mau Escarpment, Cherangani Hills, and Mt. Elgon regions of western Kenyan as a new and distinct species. Other specimens from the same highland regions had been variously provisionally assigned to *Praomys* (*Hylomyscus*) *denniae vulcanorum* (Bishop 1979) and *H*. cf. *anselli* (Carleton et al. 2006) pending additional collecting enabling detailed morphological comparisons.

Hylomyscus kerbispeterhansi, new species

Praomys (*Hylomyscus*) *denniae vulcanorum*: Bishop, 1979:528; part.

Hylomyscus denniae: Clausnitzer and Kityo, 2001:101; part.

Hylomyscus anselli: Carleton, 2006:310; part.

Holotype.—Field Museum of Natural History, Division of Mammals catalogue number 210017 (field number TCD 2924), collected 25 July 2010 by T. Demos during a faunal survey of the Mau Escarpment, Kenya. The specimen, an adult female, was fixed in 10% formalin solution and subsequently transferred to 70% ethanol. The skull was extracted from the fluid specimen and cleaned and is in excellent condition (Fig. 2). The specimen has full adult dentition and fusion of basisphenoid–basioccipital sutures. External measurements were made in the field and include: total length, 234 mm; head and body length, 95 mm; tail length, 139 mm; hind-foot length, 20 mm; ear length, 19 mm; and body mass, 24.5 g. This specimen was included in all morphometric and molecular analyses. An aliquot of muscle tissue was taken from the specimen in the field and preserved in dimethylsulfoxide prior to final cryogenic storage at −180°C at FMNH.

Type locality.—Kenya, Rift Valley Province, Narok District, Mau Escarpment, 15.5 km N, 16.4 km E Bomet, 0.64170°S, 35.49104°E, 2,350 m elevation.

Paratypes.—Three males, FMNH 209997, 210001, and 210018, and 3 females, FMNH 210000, 210015, and 210040, all collected during 22–25 July 2010 at the type locality are deposited in the FMNH. All specimens were fixed in 10% formalin and subsequently preserved in 70% ethanol, with crania extracted and cleaned. Muscle tissue samples were preserved in dimethylsulfoxide in the field and subsequently stored at −180°C at FMNH. Identification of all paratypes was confirmed by *Cytb* molecular sequence data.

Fig. 2.—Dorsal, ventral, and lateral views of the cranium of *Hylomyscus kerbispeterhansi*, new species (holotype FMNH 210017).

Additional specimens.—To morphometrically delineate the new taxon and study its genetic variability numerous other specimens of *Hylomyscus* from the *H. anselli* and *H. denniae* groups from the type locality and other East African localities were included in our analyses. Representative skulls for comparison are provided in Fig. 3. Summary statistics for univariate mensural variables are provided in Table 1. These additional specimens examined are listed in Appendix I.

Diagnosis.—A member of the *H. anselli* group as characterized by the absence of 1 pectoral pair of teats (mammae total = 6), conspicuously shorter incisive foramina, and larger subsquamosal fenestrae with more slender hamular process relative to members of the *H. denniae* group (*denniae*, *endorobae*, and *vulcanorum*—sensu Carleton and Stanley 2005). Subsquamosal fenestrae are larger than in other members of the *H. anselli* group. *H. kerbispeterhansi* is intermediate in the majority of cranial measurements between relatively smaller *H. arcimontensis* and relatively larger *H. anselli* including zygomatic breadth, length of nasals, postpalatal length, width of M1, and crown length of upper toothrow (Table 1).

Comparisons.—*Hylomyscus kerbispeterhansi* is larger than *H. arcimontensis* in key cranial measures: zygomatic breadth,

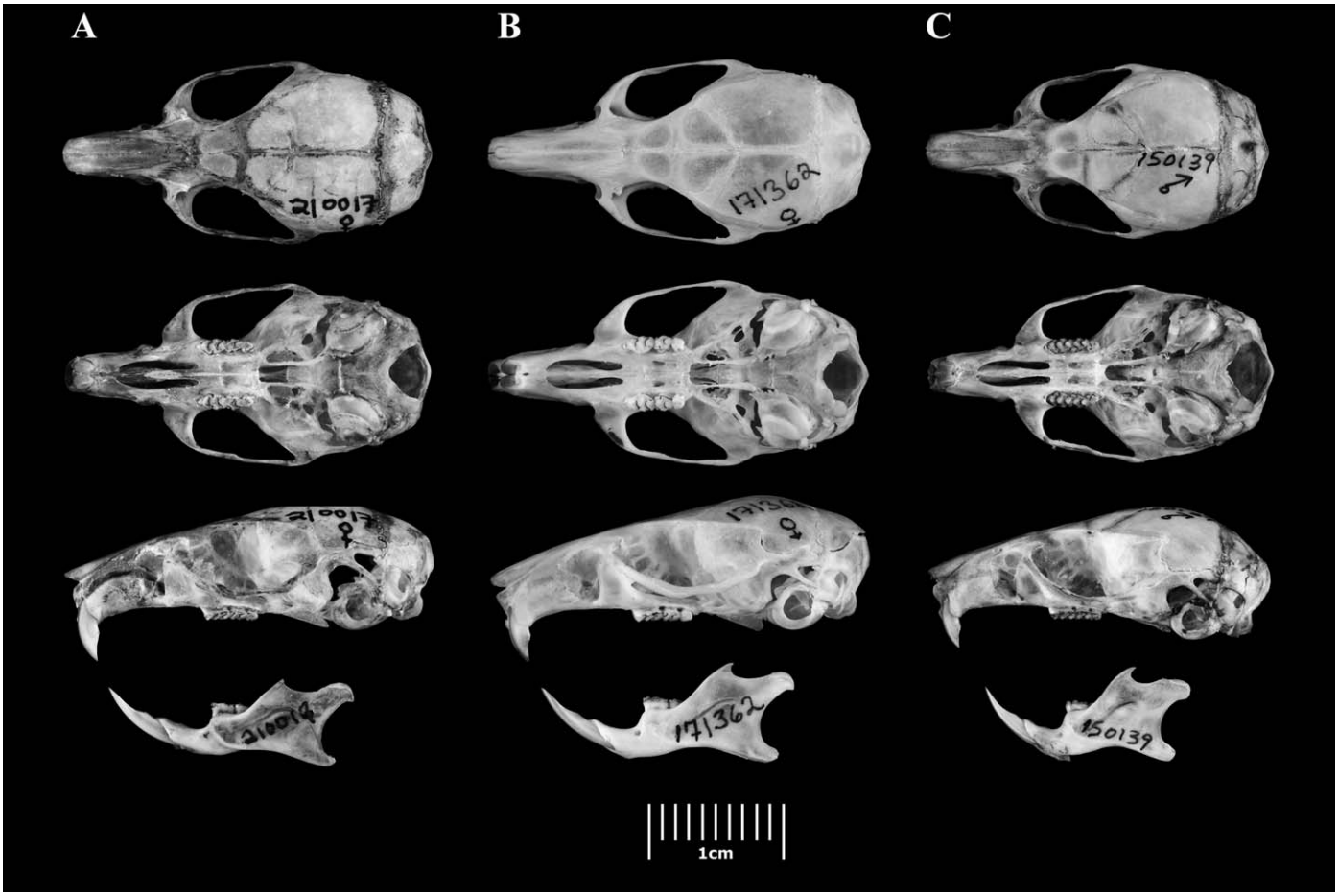

Fig. 3.—Dorsal, ventral, and lateral views of crania of *Hylomyscus*: A) *H. anselli* (FMNH 171346; occipitonasal length [ONL] = 27.3 mm), a male from Mbizi Mountains, Tanzania; B) *H. kerbispeterhansi*, new species (FMNH 210017 [holotype]; ONL = 26.7 mm), a female from Mau Escarpment, Kenya; and C) *H. endorobae* (FMNH 209996; ONL = 27.87), a female from Mau Escarpment, Kenya.

length of incisive foramina, length of diastema, and length of auditory bullae (Table 1). Differences with *H. anselli* are more subtle, although *H. kerbispeterhansi* is generally smaller in most cranial and external measures. The crown length of upper toothrow of *H. kerbispeterhansi* is shorter and its range is nonoverlapping with *H. anselli* (3.6–3.93 mm versus 3.97–4.51 mm). *H. kerbispeterhansi* has smaller and more anteriorly situated posterior palatal foramina that are located between M1 and M2 , which are not visible in ventral view, but can be seen in lateral or oblique views. In *H. anselli* the posterior palatal foramina are much larger, are readily visible in ventral view, and continue posteriorly across the anterior one-third of the M2 (Fig. 3); in *H. kerbispeterhansi*, the frontoparietal suture is very broadly U-shaped, whereas in *H. anselli* this suture is more V-shaped; in *H. kerbispeterhansi*, the subsquamosal fenestra is larger and the postglenoid foramen is more arched compared to in *H. anselli*; in *H. kerbispeterhansi*, the zygomatic plate is more orthogonal (less sinuous) than in *H. anselli* (in the new species, the plate may even be slanted slightly backward, whereas in *H. anselli*, it often bulges forward with a more rounded profile); incisive foramina are wider in center in *H. kerbispeterhansi* compared to *H. anselli* and mesopterygoid fossa is more constricted medially in *H. kerbispeterhansi* in comparison to *H. anselli*, which lacks any narrowing along fossa length.

Description.—Pelage soft and fine in texture, rather long (8–10 mm over middle rump) and close-lying. Dorsal body hairs dark slate gray over most of their length with medium brownish red tips; pelage grades to lighter rufous brown along flanks; guard hairs blackish brown and distinctly longer than body fur of lower dorsum. Ventral pelage appears whitish gray; basal one-half medium gray and distal one-half white. Young specimens are blackish gray. Tail distinctly longer than head and body (TAIL = 148% ± 11.2% of HB); color dark chocolate brown; caudal scales finely textured and hairs short, about 1.5–2 annuli in length; tail appears naked over most of its length, fine hairs becoming longer and brighter toward the tip. Pinnae dark brown. Hind feet short and narrow; 5 digits; plantar surface naked, with 6 well-formed pads. In the forefeet, the 5th digit is long, approximately equal to digits 2–4. Tops of forefeet and hind feet are covered with short, light brown hair; claws are covered by white tufts of hair. There are 6 mammae distributed as 1 axial and 2 inguinal pairs.

Table 1.—External and craniodental descriptive statistics (mean, ± 1 *SD*, and range; see "Materials and Methods" for definitions of abbreviations) for *Hylomyscus kerbispeterhansi*, *H. anselli*, *H. arcimontensis*, and *H. endorobae*. Measurements are in millimeters, except WT, which is in grams.

Variable	*H. kerbispeterhansi*	*H. anselli*	*H. arcimontensis*	*H. endorobae*
TOT	227 ± 13.8, 196–260	246 ± 7.4, 238–264	223 ± 11.8, 190–249	246 ± 13.4, 217–276
HB	92 ± 5.9, 80–103	101 ± 7.4, 95–109	90 ± 5.7, 80–105	102 ± 8.8, 83–121
TAIL	136 ± 10.3, 108–158	146 ± 5.0, 141–159	134 ± 7.3, 110–151	144 ± 7.1, 127–155
HF	20 ± 0.9, 18–22	21 ± 0.7, 20–22	20 ± 1.0, 18–22	122 ± 1.1, 20–25
EAR	20 ± 1.1, 17–22	20 ± 0.5, 19–21	18 ± 1.0, 16–21	19 ± 1.3, 16–22
WT	23.9 ± 4.8, 16–39	28.5 ± 3.1, 22.0–34.5	19.0 ± 4.0, 13.5–28.5	28.4 ± 5.5, 18–37.5
ONL	26.2 ± 0.8, 24.5–28.0	27.0 ± 0.6, 25.8–28.5	25.0 ± 0.9, 23.0–26.4	27.6 ± 0.9, 25.7–29.7
ZB	13.1 ± 0.4, 12.2–14.2	13.3 ± 0.2, 12.5–14.0	12.5 ± 0.4, 11.6–13.2	13.6 ± 0.5, 12.5–14.5
BBC	11.8 ± 0.3, 11.2–12.5	12.1 ± 0.2, 11.2–12.5	11.3 ± 0.3, 10.7–12.0	12.4 ± 0.4, 11.5–13.2
BOC	6.1 ± 0.2, 5.6–6.5	6.1 ± 0.1, 5.9–6.3	5.9 ± 0.3, 5.2–6.3	6.0 ± 0.1, 5.7–6.4
LOB	4.3 ± 0.1, 4.2–4.6	4.6 ± 0.1, 4.4–4.9	4.2 ± 0.1, 4.0–4.4	4.3 ± 0.1, 4.0–4.6
BR	4.5 ± 0.3, 4.1–5.6	4.6 ± 0.1, 4.3–5.0	4.2 ± 0.2, 3.8–4.7	4.7 ± 0.2, 4.3–5.1
PPL	8.9 ± 0.5, 7.1–10.3	9.3 ± 0.3, 8.7–10.1	8.6 ± 0.4, 7.4–9.6	9.6 ± 0.5, 8.5–10.7
LBP	4.5 ± 0.2, 3.9–4.8	4.8 ± 0.2, 4.4–5.1	4.3 ± 0.2, 4.0–4.7	4.3 ± 0.2, 3.9–4.8
LIF	5.5 ± 0.3, 4.9–6.1	5.4 ± 0.2, 5.0–5.8	5.0 ± 0.2, 4.6–5.5	6.2 ± 0.2, 5.8–6.7
LD	7.7 ± 0.4, 7.1–8.6	7.5 ± 0.2, 7.0–8.0	7.0 ± 0.3, 6.4–7.5	7.6 ± 0.3, 7.0–8.0
BZP	2.4 ± 0.1, 2.1–2.8	2.3 ± 0.2, 2.1–2.6	2.2 ± 0.1, 2.0–2.4	2.4 ± 0.1, 2.0–2.7
LAB	4.6 ± 0.2, 4.1–4.9	4.5 ± 0.1, 4.3–4.7	4.1 ± 0.1, 3.7–4.3	4.6 ± 0.2, 4.3–4.9
CLM	3.8 ± 0.1, 3.6–3.9	4.1 ± 0.1, 4.0–4.5	3.7 ± 0.1, 3.4–3.9	4.2 ± 0.1, 3.8–4.5
WM1	1.2 ± 0.05, 1.2–1.3	1.3 ± 0.04, 1.2–1.3	1.1 ± 0.05, 1.1–1.2	1.3 ± 0.07, 1.1–1.4

The skull is delicate overall as in other members of the *H. anselli* group (Carleton and Stanley 2005) and characterized by small size, short rostrum, and thin zygomatic plates. The braincase is smooth and distinctly arched over parietals. Rostral processes of premaxillaries terminate approximately equal with the rear border of the nasals; interorbital breadth relatively narrow, lacking supraorbital ridging or beading (as in *H. aeta*). Zygomatic plate medium in width; dorsal notch is shallow. Hard palate smooth, slightly concave dorsally; posterior palatal foramina lie between the rear of M1 and front of M2. Ectotympanic bullae moderately inflated for the genus. Upper incisors enamel face yellow-orange. Upper molar row about as long as the hard palate and toothrows parallel. Incisive foramina moderately long (LIF = 71% ± 3.5% of LD), posteriorly terminating just short of or equal to the anterior root of the 1st molars; foramina broad over their anterior portion, more strongly constricted over posterior one-half. Mesopterygoid fossa is constricted medially in comparison to both *H. anselli* and *H. arcimontensis*.

Phylogenetically, the new species is distinguished as reciprocally monophyletic from other members of the *H. anselli* group based on mitochondrial *Cytb* and 3 autosomal intron (ABHD, ACOX2, and GAD2) sequence data. *H. kerbispeterhansi* is strongly supported as sister to *H. anselli* (*H. arcimontensis* (*H. kerbispeterhansi*, *H. anselli*)).

Ecology and reproduction.—All specimens of *H. kerbispeterhansi* were collected in forested habitats above 2,300 m in elevation. Activity is strictly nocturnal because all were collected during morning trap checks (approximately 0700–0800 h). The arboreal habits of this climbing mouse are not well documented, although arboreal habits have been documented for other *Hylomyscus* species (Stanley et al. 1998; Nicolas et al. 2008). Although most commonly captured in traps placed on the ground, 22 of 152 specimens were captured in traps set 1–2 m off the ground on vines and tree limbs. Specimens from Mau Escarpment were collected during 2010 from a variety of forested habitats including well-drained closed-canopy montane forest (2,350 m), selectively logged montane forest (2,300–2,360 m), montane secondary forest with bracken (2,320 m), and in dense undergrowth alongside montane forest streams (2,210–2,320 m). *H. kerbispeterhansi* is sympatric with *H. endorobae* in the western Mau Escarpment and they were found to be syntopic in several traplines where both species were captured in the same station. *Hylomyscus* species were the 3rd most abundant rodent species in the Mau forest after *Praomys jacksoni* and *Lophuromys aquilus* based on 1,505 trap-nights. No specimens of *H. endorobae* were collected during 2,400 trap-nights of collecting in Mt. Elgon or 700 trap-nights in Cherangani Hills, strongly suggesting that the ranges of *H. kerbispeterhansi* and *H. endorobae* overlap only in the Mau Escarpment in what may be a zone of secondary contact. Thus, *H. kerbispeterhansi* is limited to Kenya's western montane blocks (Mt. Elgon and Cherangani Hills), whereas the eastern montane blocks (Mt. Kenya and Aberdare Mts.) house only *H. endorobae*. Extensive surveys by TCD, BA, and colleagues of the aforementioned east Kenyan montane forests have uncovered no presence of *H. kerbispeterhansi* east of the Kenyan Rift Valley. Surveys of the Cherangani Hills and Mt. Elgon in 2011 found *H. kerbispeterhansi* in primary montane forest (2,740 m, Cherangani Hills), selectively logged and secondary montane forest (2,520–2,770 m, both mountains), and in mixed bamboo–*Hagenia* forest (2,540 m, Mt. Elgon). In both of these disjunct montane forests *H. kerbispeterhansi* was the most abundant rodent species, comprising 44% and 42% of terrestrial rodents recorded, respectively. An extensive survey

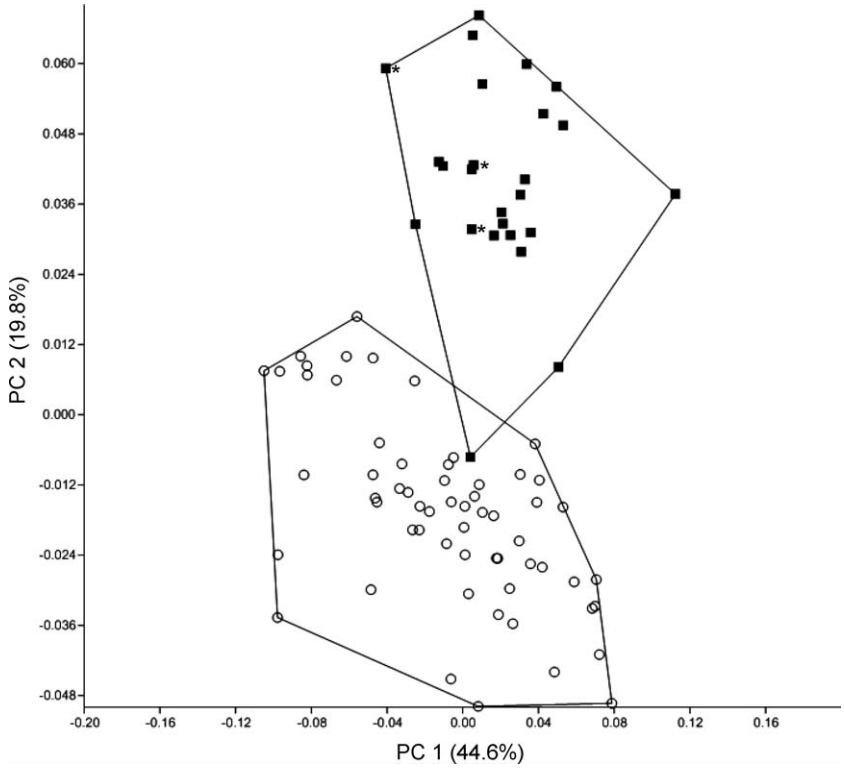

Fig. 4.—Scatter plot of principal component analysis (PCA) performed on 14 log-transformed craniodental measurements. The filled squares represent specimens of *Hylomyscus anselli* from the Mbizi Mts., Tanzania; the unfilled circles represent specimens of *H. kerbispeterhansi* from western Kenya; and the 3 asterisks (*) represent specimens from Bishop's (1979) type series of *Praomys* (*Hylomyscus*) *denniae anselli* from Zambia.

at a 2nd higher-elevation camp on Mt. Elgon (3,000–3,180 m) did not record any *Hylomyscus* specimens during 1,138 trap-nights in a variety of microhabitats that included upper montane forest–alpine grassland mosaics, *Hagenia* groves, and gallery forest along the Kimothon River.

Among 8 adult females examined for reproductive condition 3 were pregnant, with the number of embryos in a single uterine horn ranging from 1 to 4 and the number for both horns combined ranging from 3 to 5, with an average litter size of 4. The embryos averaged 14.7 mm in crown–rump length (range = 12–18 mm). Among 9 adult males examined, testes averaged 14 mm in length (range = 8–19 mm) and 6.9 mm in width (range = 4–9 mm).

Etymology.—The new species is named in honor of Julian Kerbis Peterhans, in recognition of his significant contributions to current knowledge on African small mammals, his generosity in sharing data and specimens resulting from his extensive fieldwork, as well as his ongoing efforts in promoting African conservation and education.

Distribution.—*Hylomyscus kerbispeterhansi* is currently known from tropical montane forests of the Mau Escarpment, Cherangani Hills, and Mt. Elgon in Kenya, with an elevational range of 2,320–2,740 m. Although not presently recorded from Ugandan slopes of Mt. Elgon, we presume it is distributed in these montane forests, which are continuous with those on the Kenyan slopes of Mt. Elgon.

Nomenclatural statement.—An LSID number was obtained for the new species (*Hylomyscus kerbispeterhansi*): urn:lsid:zoobank.org:pub:2E2A198B-70AB-49EF-98D5-2CE0240002D4.

Morphometrics.—A principal component analysis was performed on 14 log-transformed craniodental variables for specimens of *H. kerbispeterhansi* and *H. anselli* with the 2 taxa occupying mostly discrete regions of multivariate space (Fig. 4). Results of a discriminant function analysis of 14 log-transformed craniodental variables for specimens of *H. kerbispeterhansi*, *H. anselli*, *H. arcimontensis*, and *H. endorobae* are summarized in Fig. 5. Multivariate ordinations performed on the 1st and 2nd canonical variates (CV1 and CV2) accounted for 85% of the cumulative proportion of variation for skull characters and showed well-defined morphometric structure with moderate overlap in multivariate space among specimens assigned to *H. kerbispeterhansi*, *H. arcimontensis*, and *H. anselli*, and no overlap with *H. endorobae*. CV1 discriminates populations of *H. endorobae* (within the *H. denniae* group) from members of the *H. anselli* group. The standardized coefficients for canonical variables matrix indicates LD is the most important negatively correlated variable and ONL, LIF, and CLM are the most negatively correlated variables on the CV1 axis (Table 2). CV2 discriminates among species assigned to the *H. anselli* group with specimens assigned to *H. kerbispeterhansi* having marginal overlap with *H. anselli*. On the CV2 axis ONL and

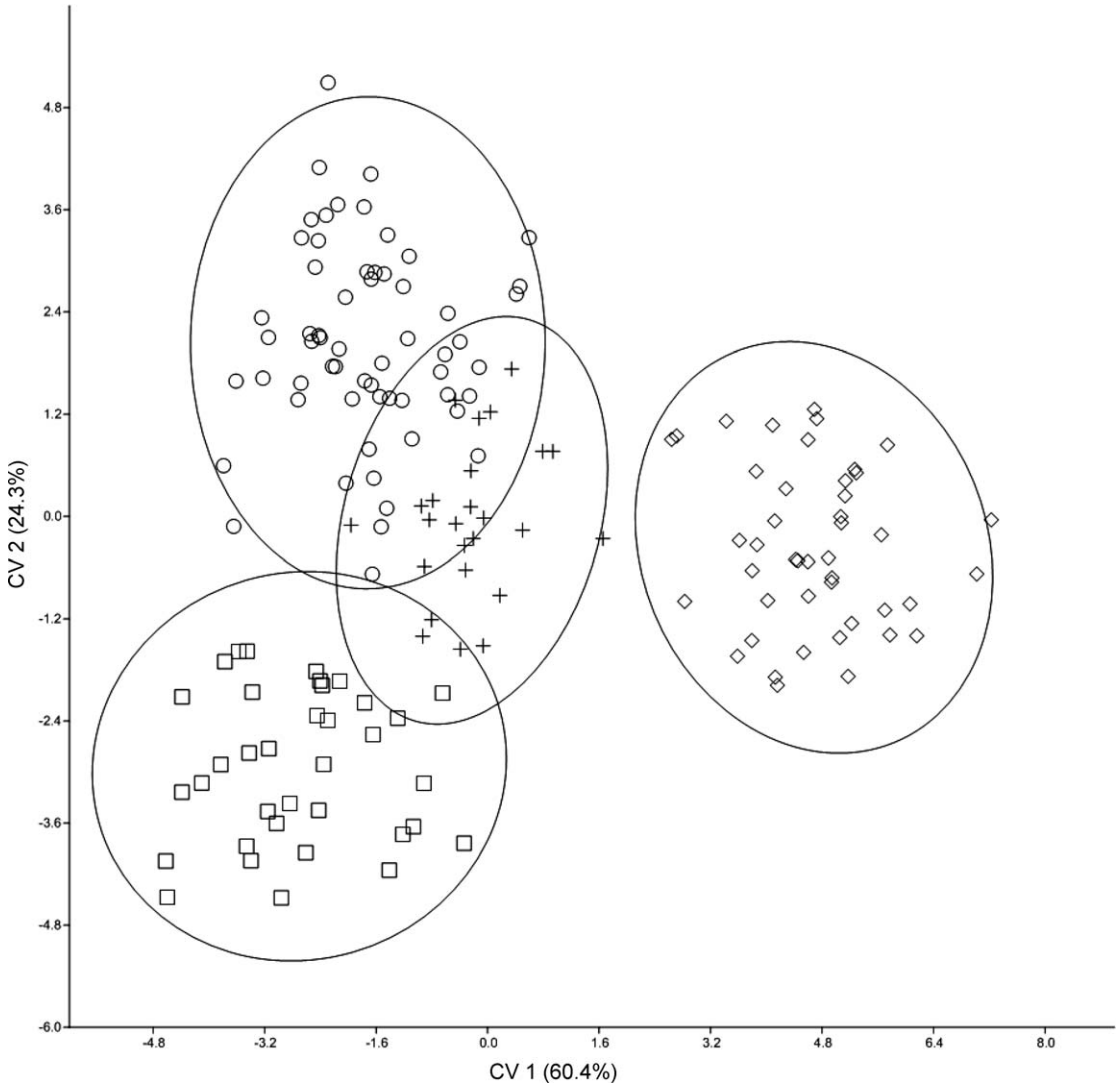

Fig. 5.—Scatter plot of canonical variates (CV) axes 1 and 2 depicting results of discriminant function analysis performed on 14 log-transformed craniodental measurements. Projection of individual specimen scores from 163 specimens assigned to 4 taxa is depicted according to the key in the plot. The 95% confidence limits for taxa are depicted by ellipses.

PPL are the most negatively correlated variables and LD and CLM are the most positively correlated variables. ONL weights heavily on CV1 and distinguishes the larger crania of *H. endorobae* from the 3 members of the *H. anselli* clade. LD weights most heavily on CV2 and discriminates most among the 3 *H. anselli* group clades. The group centroids of the 4 species showed highly significant statistical differences (Wilks' lambda = 0.007, $F_{42,440} = 45.1$, $P < 0.0001$). Squared Mahalanobis distances between species were 23.5 between *H. kerbispeterhansi* and *H. anselli*, 25.7 between *H. arcimontensis* and *H. kerbispeterhansi*, and 46.8 between *H. kerbispeterhansi* and *H. endorobae*. Dendrograms based on the Mahalanobis distance matrix and a corrected between-group genetic distance matrix using *Cytb* sequence data inferred the same topology and similar branch lengths for all 4 species (Fig. 6).

When entered as unknowns in the 4-group discriminant function analysis and classified according to posterior probabilities of group membership, 1 individual from *H. anselli* and 1 individual from *H. arcimontensis* were assigned to the incorrect species in the classification table. All specimens of *H. kerbispeterhansi* were assigned to their appropriate taxonomic cluster.

Species-tree inference and Bayesian species delimitation.—The 3 autosomal introns we sequenced for *H. denniae*, *H. anselli*, and *H. stella* had between 31 and 78 segregating sites, whereas the mtDNA *Cytb* locus had 278 segregating sites. All 3 of the independent gene trees for the nuclear loci support populations of *H. kerbispeterhansi* from west-central Kenya as a reciprocally monophyletic group, distinct from species within the *H. anselli* and *H. denniae* species groups. The mtDNA gene tree strongly supports *H. kerbispeterhansi* as monophyletic with little divergence between populations from Mau Escarpment, the Cherangani Hills, and Mt. Elgon as distinct (Supporting Information S1, DOI: 10.1644/13-MAMM-A-268.S1). Mean between-group genetic distances (Kimura 2-parameter) for *Cytb* are 3.2% between *H. kerbispeterhansi*

Table 2.—Results (correlations) of discriminant function analysis performed on the operational taxonomic units representing *Hylomyscus kerbispeterhansi*, *H. anselli*, *H. arcimontensis*, and *H. endorobae* ($n = 165$). Variables are the measurements as defined in the "Materials and Methods." CV = canonical variate. Variables highlighted in boldface type are discussed in the text.

	Correlations	
Variable	CV1	CV2
ONL	**0.71**	**−0.67**
ZB	0.14	−0.18
BBC	0.26	0.19
BOC	−0.45	0.13
LOB	−0.44	−0.01
BR	0.32	−0.14
PPL	−0.19	**−0.92**
LBP	−0.42	0.08
LIF	**0.55**	0.19
LD	**−0.78**	**1.46**
BZP	−0.18	0.05
LAB	0.22	**0.57**
CLM	**0.57**	0.10
WM1	0.14	0.15
Eigenvalues	8.7	3.5
Cumulative % variance	60.4	84.7
Canonical correlations	0.95	0.88

and *H. anselli* and 7.4% between *H. kerbispeterhansi* and *H. arcimontensis* (Table 3). Distances between species assigned to the *H. anselli* group and *H. endorobae* from the *H. denniae* group range from 15.3% to 16.0%. Additional Kimura 2-parameter genetic distances are given for 3 introns in Table 3.

The *BEAST species-tree analysis strongly supports *H. kerbispeterhansi* as sister to *H. anselli* and *H. anselli* + *H. kerbispeterhansi* as sister to *H. arcimontensis* (Fig. 7). The species tree also recovers those clades delimited as species on the basis of morphometric and morphological analyses in revisions of the *H. anselli* and *H. denniae* groups (Carleton and Stanley 2005; Carleton et al. 2006) with posterior probabilities of 100%. The topology of the 3 members of the *H. denniae* group is not well resolved, with < 70% support for *H. vulcanorum* as sister to *H. endorobae*.

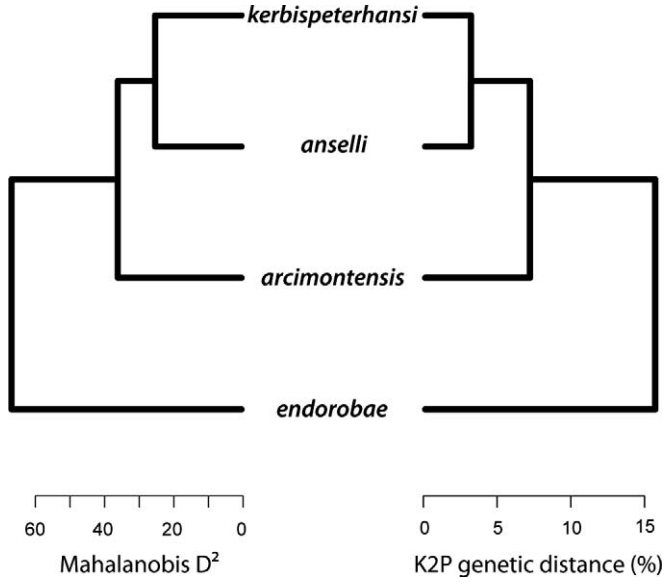

Fig. 6.—Cluster analysis based on Mahalanobis distances between taxa (left) and corrected cytochrome-*b* (*Cytb*) net between-taxa genetic distances (right). Both dendrograms recover the same topology and similar branch lengths based on independent morphometric and genetic data sets.

Table 3.—Corrected (Kimura 2-parameter) within and between group distances calculated for mitochondrial DNA (cytochrome-*b* [*Cytb*]) and nuclear intron (ABHD11-5, ACOX2-3, and GAD2-1) sequence data for 4 species of *Hylomyscus*.

Species	*Cytb*	ABHD11-5	ACOX2-3	GAD2-1
kerbispeterhansi	0.002	0.002	0.000	0.000
anselli	0.000	0.001	0.000	0.000
arcimontensis	0.001	0.001	0.000	0.000
endorobae	0.001	0.002	0.001	0.004
kerbispeterhansi versus *anselli*	0.032	0.005	0.009	0.006
kerbispeterhansi versus *arcimontensis*	0.074	0.008	0.006	0.011
kerbispeterhansi versus *endorobae*	0.153	0.016	0.040	0.043
anselli versus *arcimontensis*	0.071	0.006	0.009	0.013
anselli versus *endorobae*	0.157	0.012	0.044	0.047
arcimontensis versus *endorobae*	0.160	0.018	0.040	0.041

The Bayesian species delimitation results also are indicated on Fig. 7 and support the *H. anselli* group as comprising 3 species that includes the new species with speciation probabilities of 1.0 at relevant nodes. The 3 clades referred as species by Carleton and Stanley (2005) from the *H. denniae* group also are supported, with speciation probabilities of 1.0. We emphasize that these species delimitations were applied to taxa on the basis of populations assigned to individual mountain ranges (e.g., Itombwe Mountains, Cherangani Hills, and Mt. Kenya), and that we did not a priori designate species to the guide tree required by BPP at the species level for those clades distributed across multiple mountain ranges (e.g., *H. endorobae* distributed across 3 mountain ranges). We consider this to be a conservative approach because we are not biasing assignment of populations to species, but instead relying on statistical measures of support for lineages based on the results of the species-tree analysis (Leaché and Fujita 2010; Camargo et al. 2012). When populations were a priori assigned to species the same Bayesian species delimitations were recovered.

Historical demography.—Summary statistics from *Cytb* sequence data (1,119 base pairs) indicate a similar number of haplotypes (h) in *H. kerbispeterhansi* ($h = 12$) as in *H. endorobae* ($h = 14$). The numbers of individuals and localities also are similar between the 2 samples: *H. kerbispeterhansi*, $n = 41$ individuals from 4 unique localities on 3 mountains; and *H. endorobae*, $n = 25$ individuals from 5 unique localities on 3 mountains. Haplotype diversity was approximately equal for both taxa ($H_d = 0.900$ in *H. kerbispeterhansi* and $H_d = 0.870$ in *H. endorobae*), whereas nucleotide diversity was low for both taxa with $\pi = 0.0026$ and 0.0019 for the respective species. Extended Bayesian skyline coalescent analyses, based on 5

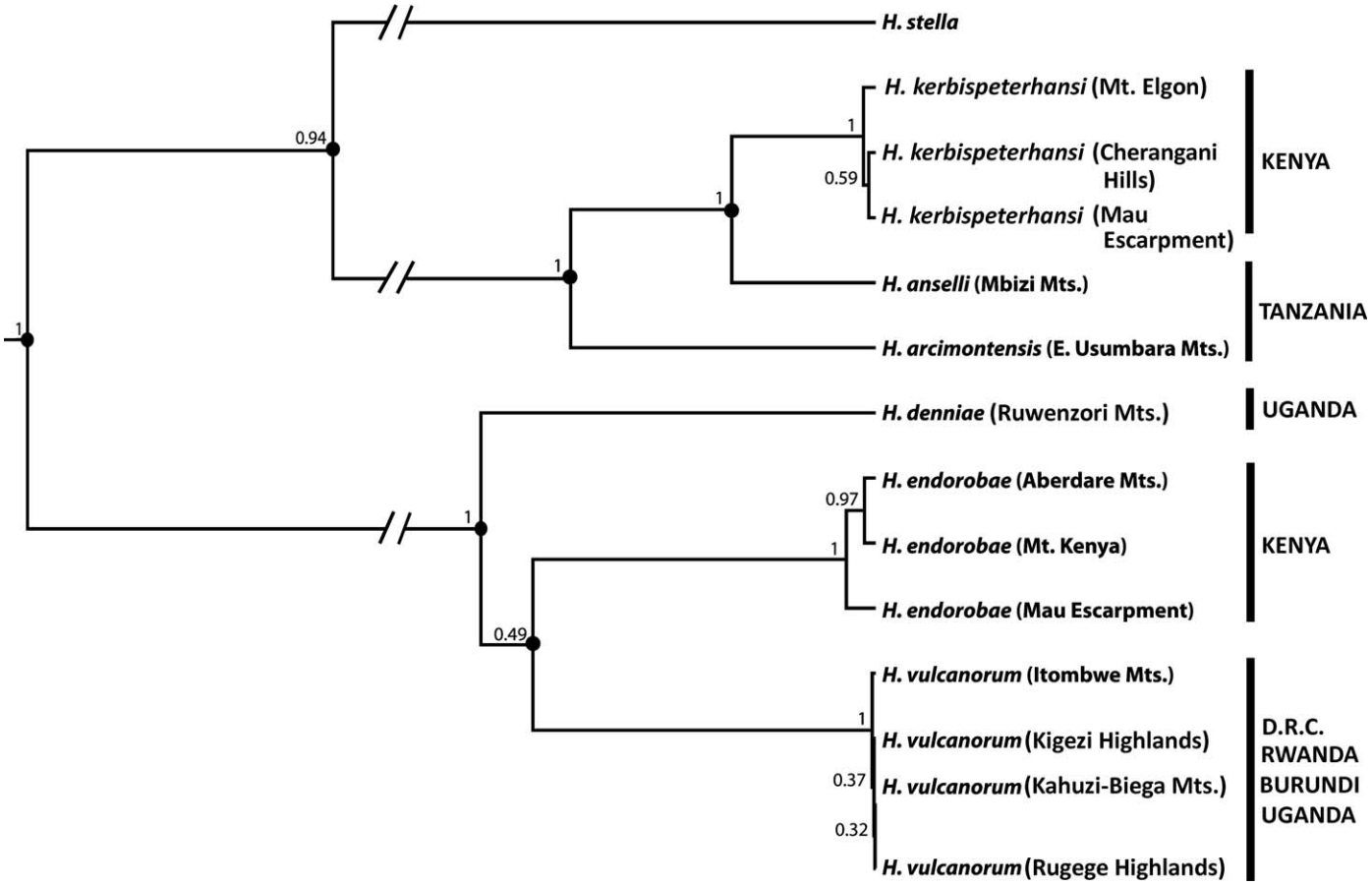

Fig. 7.—Species tree inferred in *BEAST using multilocus sequence data for 7 species of *Hylomyscus* from the *H. alleni*, *H. anselli*, and *H. denniae* species groups (Carleton et al. 2006). Numbers above branches represent Bayesian posterior probability values and filled circles on nodes indicate speciation probabilities ≥ 0.99 for Bayesian species delimitation analysis in Bayesian Phylogenetics and Phylogeography (BPP).

nuclear intron loci and the *Cytb* locus, for populations across Kenya, support population and geographic expansion dating 10,000–20,000 years ago for *H. kerbispeterhansi* and from ~100,000 years ago for *H. endorobae*, although with wide 95% highest posterior density intervals (Fig. 8). Our sampling strategy of combining populations (demes) from across Kenya within each species for skyline analysis has been shown to minimize false inferences of demographic change (Heller et al. 2013). This pattern is broadly coincident with Pleistocene forest refugial fragmentation during the last glacial maxima and subsequent refugial expansion after the last glacial maxima.

Results from a species-tree chronogram place the divergence between the *H. anselli* and *H. denniae* groups broadly within the Miocene (approximately 7.4 mya) and between *H. anselli* and *H. kerbispeterhansi* within the middle to late Pleistocene (approximately 0.83 mya [Supporting Information S2, DOI: 10.1644/13-MAMM-A-268.S2]). The split between *H. anselli* from southwestern Tanzania and *H. kerbispeterhansi* from the western Kenyan Highlands is broadly coincident with the intensification of global glacial climatic cycling and the intense aridification of Africa that commenced approximately 1 mya (deMenocal 2004; Anhuf et al. 2006).

Discussion

Results from independent data sets of multilocus mitochondrial and autosomal sequence data and morphometric data support recognition of a 3rd member of the *H. anselli* species group, which along with the *H. denniae* group is restricted to south-central and eastern African wet montane forests. The 3 members of the *H. anselli* complex are externally cryptic but are distinguishable on the basis of qualitative skull morphology, multivariate craniodental morphometrics, and genetics. Further work on the isolated and disjunct populations of *Hylomyscus* from the central Highlands of Angola is required to assess the distinctness of these populations tentatively assigned to the *H. anselli* group (Carleton and Stanley 2005).

The Mau region is the type locality for *H. endorobae* (Heller 1910) and Carleton et al. (2006) suggest that additional collecting, especially along elevational transects, might reveal that the 2 specimens they had examined that were assignable to the *H. anselli* group were indicative of sympatric distribution elsewhere within the region. The Mau Escarpment is strongly supported as a zone of secondary contact following allopatric speciation in the ancestor of *H. kerbispeterhansi* and *H. endorobae*. There is no evidence for hybridization in the zone

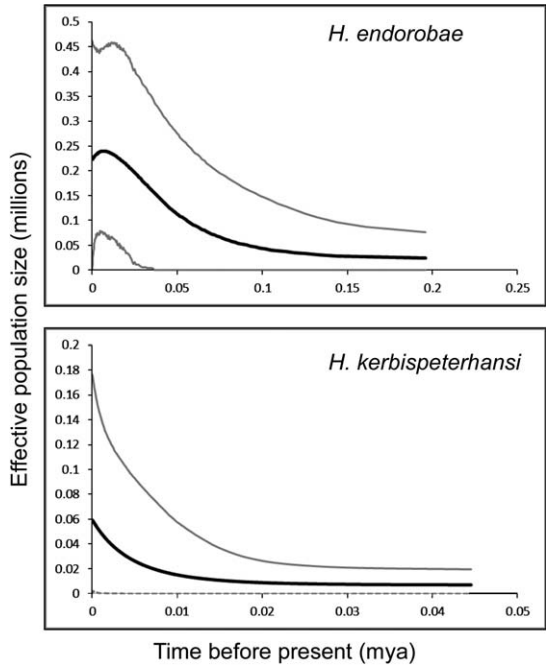

Fig. 8.—Extended Bayesian skyline plot depicting changes in effective population size (N_e) over time before present based on mitochondrial DNA (cytochrome-*b* [*Cytb*]) and nuclear DNA intron (ABHD11-5, ACOX2, ACPT-4, GAD2-1, and JMJD) sequence data. The black center line indicates the median population size and the bounding gray lines indicate the 95% highest posterior density (HPD). Both taxa show recent population expansion, although expansion in *Hylomyscus kerbispeterhansi* commenced later than in *H. endorobae*. The present N_e of *H. endorobae* is inferred to be ~5 times larger than that of *H. kerbispeterhansi*.

of sympatry as well as incompatible phenotypes (e.g., female *H. kerbispeterhansi* have 3 pairs of teats and *H. endorobae* have 4 pairs). Intensive and geographically extensive small mammal surveys of all of the isolated mountain blocks of northeastern and northwestern Tanzania have not documented the presence of any members of genus *Hylomyscus*, thus a significant geographic gap occurs in the distribution of this genus across the Northern Highlands of Tanzania (Carleton and Stanley 2012). Rather, montane forests in these highland regions contain a high abundance of *Praomys*, a genus that is widely codistributed with *Hylomyscus* across the Kenyan Highlands, Albertine Rift, central and southern Eastern Arc Mountains, southwestern Tanzanian Highlands, and the Malawi Rift. The application of standardized trapping protocols, as well as repeated faunal surveys of Tanzanian montane forests along the Tanzania–Uganda–Kenya border, strongly support the conclusion that populations of *Hylomyscus* were never present in this region or have become locally extirpated.

A pronounced disparity in population densities between *H. kerbispeterhansi* and *H. endorobae* at the 2 sites surveyed within the Mau Escarpment is suggestive of interspecific competition between these taxa. Of 69 specimens of *Hylomyscus* collected in the course of fieldwork at these 2 localities, 30 specimens had tissues taken that were sequenced for molecular analysis and of these 24 are assignable to *H. kerbispeterhansi* and 6 to *H. endorobae*. Although the documentation of a syntopic distribution for these 2 lineages on the basis of both taxa being collected along the same traplines and at the same trap stations would seem to support niche divergence facilitating coexistence, the 4:1 ratio of specimens of *H. kerbispeterhansi* to *H. endorobae* suggests that *H. kerbispeterhansi* may be competitively superior to *H. endorobae*. Additional surveys of microhabitats in the region, diet studies, and larger sample sizes would test this hypothesis. However, based on current data, we find no evidence for spatial or temporal partitioning of habitat of any kind. Although recent fieldwork conducted on Mt. Elgon in 2010 and 2011, using identical field protocols to those in Mau, did not document any *Hylomyscus* at elevations above 2,810 m (B. Agwanda, pers. obs.; T. C. Demos, pers. obs.), examination of data from previous elevational transects carried out from 2,900 to 4,200 m along the western slopes of Mt. Elgon indicates that *Hylomyscus* is present at up to 3,100 m and *Praomys* occurs at elevations up to 3,200 m (Clausnitzer 2001; Clausnitzer and Kityo 2001).

There are multiple lines of evidence that the strength of topographic relief in Kenya increased during the Pliocene–Pleistocene through extension of the African Rift into eastern Africa (Taylor et al. 2009 and references therein). During this same period pronounced intervals of aridification at approximately 2.8, 1.7, and 1.0 mya are hypothesized to have resulted in significant rain-forest contraction and fragmentation across tropical Africa (deMenocal 2004). These orogenic and climatic forces may have driven allopatric speciation in these forest-restricted montane rodents.

The geographical range of *H. kerbispeterhansi* west of the Gregory Rift in Kenya confirms suggestions by Carleton and Stanley (2005) that specimens of *Hylomyscus* from the Mau Escarpment and Mt. Elgon may have been assignable to the *H. anselli* group. Affinities between *Hylomyscus* from the Cherangani Hills and Mt. Elgon to *H. anselli* on the basis of skull size were noted by Bishop (1979); nonetheless, he referred specimens from these mountains to *H. d. vulcanorum*. The northern range extension to the western Kenyan Highlands of a 3rd member of the *H. anselli* species group, previously known to be restricted to southwestern Tanzania and Zambia, as well as the presumed absence of *H. endorobae* from the Cherangani Hills and Mt. Elgon on the basis of surveys to date, contributes to an increasing understanding of biogeographic affinities among small mammal taxa of western montane Kenya and Mt. Elgon. Kerbis Peterhans et al. (2009) noted that Mt. Elgon was inhabited by a small mammal fauna with phylogenetic affinities to the Albertine Rift and Congo Basin to the west, the Kenyan Highlands east of the Gregory Rift, and the Northern Highlands and Eastern Arc Mountains of Tanzania to the south. Carleton and Stanley (2012) present strong evidence for the lack of any *Hylomyscus* species inhabiting the Northern Highlands of Tanzania despite their proximity to the Eastern Arc Mountains, where *H. arcimon-*

tensis is broadly distributed. The approximately 900-km gap that exists between Mau Escarpment populations of *H. kerbispeterhansi* and the northernmost known population of *H. anselli* from the Ufipa Plateau of southwestern Tanzania is striking. Repeated surveys of montane forests of western Tanzania north of the Ufipa Plateau have not revealed the presence of any *Hylomyscus* species. Thus, a significant gap exists in the range of members of the *H. anselli* group to the south of Kenya as well as a disjunct distribution in members of the *H. denniae* group from the Albertine Rift with *H. endorobae* to the east. Additional surveys should reveal whether *H. endorobae* is indeed limited to sympatry with *H. kerbispeterhansi* in Mau forests and if the disparity in abundance between the 2 species is a prevalent pattern through their sympatric distribution.

Nomenclatural Statement

This article conforms to the International Code of Zoological Nomenclature as an electronic publication. This electronic work represents an immutable copy published in a journal with an ISSN number and has been archived in the following digital repositories: LOCKSS and Portico. This published work and the nomenclatural acts herein have been registered in ZooBank and assigned a Life Science Identifier (LSID). The LSID for this publication is urn:lsid:zoobank.org:pub:2E2A198B-70AB-49EF-98D5-2CE0240002D4. The information can be accessed at http://zoobank.org/urn:lsid:zoobank.org:pub:2E2A198B-70AB-49EF-98D5-2CE0240002D4.

Acknowledgments

We thank the Kenya Forest Service, Kenya Wildlife Service, and the NMK for issuing permits and facilitating logistics that allowed small mammal surveys to be conducted in Kenya. J. Kerbis Peterhans assisted with fieldwork and provided advice on morphological characters. Access to specimens, tissues, and facilities was generously granted by FMNH. W. Stanley and J. Phelps provided much-appreciated assistance related to accessing specimens and tissue loans. Financial assistance to TCD was generously provided by the City University of New York Science Fellowship Program, National Science Foundation Doctoral Dissertation Improvement Grant, FMNH Council on Africa, the American Philosophical Society Lewis and Clark Fund, the Queens College Graduate Advisory Council, the Seymour Fogel Endowment Fund of Queens College, and a Professional Staff Congress–City University of New York Research Award to TCD and MJH. Molecular analyses were carried out at the City University of New York High Performance Computing Center operated by the College of Staten Island and funded in part by National Science Foundation grants CNS-0958379 and CNS-0855217. We thank W. Stanley, B. Patterson, J. Bates, J. Robinson, J. T. Boehm, D. Alvarado-Serrano, J. Kerbis Peterhans, and 2 anonymous reviewers for insightful comments and advice on the manuscript.

Supporting Information

Supporting Information S1.—Mitochondrial (cytochrome-*b* [*Cytb*]) Bayesian gene tree inferred for *Hylomyscus* with posterior probabilities (above node) and maximum-likelihood bootstrap values (below node). An asterisk (*) indicates node is not supported in the maximum-likelihood tree.

Found at DOI: 10.1644/13-MAMM-A-268.S1

Supporting Information S2.—Chronogram inferred for *Hylomyscus* under a relaxed molecular clock implemented in *BEAST. Nodal bars are 95% highest posterior densities for age estimates. Median node ages are indicated adjacent to nodes. The gray shading delimits the Pleistocene epoch. Arrows indicate timing of isolation of clades from the Kenyan Highlands from Albertine Rift and Tanzanian Highlands clades.

Found at DOI: 10.1644/13-MAMM-A-268.S2

Literature Cited

Anhuf, D., et al. 2006. Paleo-environmental change in Amazonian and African rainforest during the LGM. Palaeogeography, Palaeoclimatology, Palaeoecology 239:510–527.

Bishop, I. R. 1979. Notes on *Praomys* (*Hylomyscus*) in eastern Africa. Mammalia 43:521–530.

Bryja, J., et al. 2012. Revised occurrence of rodents from the tribe Praomyini (Muridae) in Zambia based on mitochondrial DNA analyses: implications for biogeography and conservation. Folia Zoologica 61:225–232.

Camargo, A., M. Morando, L. J. Avila, and J. W. Sites. 2012. Species delimitation with ABC and other coalescent-based methods: a test of accuracy with simulations and an empirical example with lizards of the *Liolaemus darwinii* complex (Squamata: Liolaemidae). Evolution 66:2834–2849.

Carleton, M. D., J. C. Kerbis Peterhans, and W. T. Stanley. 2006. Review of the *Hylomyscus denniae* group (Rodentia: Muridae) in eastern Africa, with comments on the generic allocation of *Epimys endorobae* Heller. Proceedings of the Biological Society of Washington 119:293–325.

Carleton, M. D., and W. T. Stanley. 2005. Review of the *Hylomyscus denniae* complex (Rodentia: Muridae) in Tanzania, with a description of a new species. Proceedings of the Biological Society of Washington 118:619–646.

Carleton, M. D., and W. T. Stanley. 2012. Species limits within the *Praomys delectorum* group (Rodentia: Muridae: Murinae) of East Africa: a morphometric reassessment and biogeographical implications. Zoological Journal of the Linnean Society 165:420–469.

Clausnitzer, V. 2001. Rodents of the afro-alpine zone of Mt. Elgon. Pp. 427–443 in African small mammals (C. Denys, L. Granjon, and A. Poulet, eds.). IRD Editions, Paris, France.

Clausnitzer, V., and R. Kityo. 2001. Altitudinal distribution of rodents (Muridae and Gliridae) on Mt Elgon, Uganda. Tropical Zoology 14:95–118.

Darriba, D., G. L. Taboada, R. Doallo, and D. Posada. 2012. jModelTest 2: more models, new heuristics and parallel computing. Nature Methods 9:772.

deMenocal, P. B. 2004. African climate change and faunal evolution during the Pliocene–Pleistocene. Earth and Planetary Science Letters 220:3–24.

Demos, T. C., J. C. Kerbis Peterhans, B. Agwanda, and M. J. Hickerson. 2013. Uncovering cryptic diversity and refugial persistence among small mammal lineages across the Eastern Afromontane biodiversity hotspot. Molecular Phylogenetics and Evolution http://dx.doi.org/10.1016/j.ympev.2013.10.014

Drummond, A. J., and A. Rambaut. 2007. BEAST: Bayesian evolutionary analysis by sampling trees. BMC Evolutionary Biology 7:214.

Drummond, A. J., M. A. Suchard, D. Xie, and A. Rambaut. 2012. Bayesian phylogenetics with BEAUti and the BEAST 1.7. Molecular Biology and Evolution 29:1969–1973.

Drummond, A. J., et al. 2013. Geneious Pro v6.0.5. http://www.geneious.com.

Edwards, S. V., and P. Beerli. 2000. Perspective: gene divergence, population divergence, and the variance in coalescence time in phylogeographic studies. Evolution 54:1839–1854.

Fujita, M. K., A. D. Leaché, F. T. Burbrink, J. A. McGuire, and C. Moritz. 2012. Coalescent-based species delimitation in an integrative taxonomy. Trends in Ecology & Evolution 27:480–488.

Guindon, S., and O. Gascuel. 2003. A simple, fast and accurate method to estimate large phylogenies by maximum-likelihood. Systematic Biology 52:696–704.

Heller, E. 1910. Descriptions of seven new species of East African mammals. Smithsonian Miscellaneous Collections 56:1–5.

Heller, R., L. Chikhi, and H. R. Siegismund. 2013. The confounding effect of population structure on Bayesian skyline plot inferences of demographic history. PLoS ONE 8:e62992.

Hickerson, M. J., et al. 2010. Phylogeography's past, present, and future: 10 years after Avise, 2000. Molecular Phylogenetics and Evolution 54:291–301.

Igea, J., J. Juste, and J. Castresana. 2010. Novel intron markers to study the phylogeny of closely related mammalian species. BMC Evolutionary Biology 10:369.

Kerbis Peterhans, J. C., R. M. Kityo, W. T. Stanley, and P. K. Austin. 1998. Small mammals along an elevational gradient in Ruwenzori Mountains National Park, Uganda. Pp. 149–171 in The Ruwenzori Mountains National Park, Uganda (H. Osmaston and J. Nyakaana, eds.). Makerere University, Kampala, Republic of Uganda.

Kerbis Peterhans, J. C., W. T. Stanley, R. Hutterer, T. C. Demos, and B. Agwanda. 2009. A new species of *Surdisorex* Thomas, 1906 (Mammalia, Soricidae) from western Kenya. Bonner Zoologische Beiträge 56:175–183.

Leaché, A. D., and M. K. Fujita. 2010. Bayesian species delimitation in West African forest geckos (*Hemidactylus fasciatus*). Proceedings of the Royal Society, B. Biological Sciences 277:3071–3077.

Lecompte, E., K. Aplin, C. Denys, F. Catzeflis, M. Chades, and P. Chevret. 2008. Phylogeny and biogeography of African Murinae based on mitochondrial and nuclear gene sequences, with a new tribal classification of the subfamily. BMC Evolutionary Biology 8:199.

Lecompte, E., L. Granjon, J. Kerbis Peterhans, and C. Denys. 2002. Cytochrome *b*–based phylogeny of the *Praomys* group (Rodentia, Murinae): a new African radiation? Comptes Rendus Biologies 325:827–840.

Librado, P., and J. Rozas. 2009. DnaSP v5: a software for comprehensive analysis of DNA polymorphism data. Bioinformatics 25:1451–1452.

Milne I., et al. 2009. TOPALi v2: a rich graphical interface for evolutionary analyses of multiple alignments on HPC clusters and multi-core desktops. Bioinformatics 25:126–127.

Nachman, M. W., and S. L. Crowell. 2000. Estimate of the mutation rate per nucleotide in humans. Genetics 156:297–304.

Nicolas, V., and M. Colyn. 2003. Seasonal variations in population and community structure of small rodents in a tropical forest of Gabon. Canadian Journal of Zoology 81:1034–1046.

Nicolas, V., W. Wendelen, P. Barriere, A. Dudu, and M. Colyn. 2008. Morphometric variation in *Hylomyscus alleni* and *H. stella* (Rodentia: Muridae), and description of a new species. Journal of Mammalogy 89:222–231.

Nicolas, V., et al. 2011. The roles of rivers and Pleistocene refugia in shaping genetic diversity in *Praomys misonnei* in tropical Africa. Journal of Biogeography 38:191–207.

Rambaut, A., and A. J. Drummond. 2007. Tracer v1.5. http://beast.bio.ed.ac.uk/Tracer.

R Development Core Team. 2013. R: a language and environment for statistical computing. R Foundation for Statistical Computing, Vienna, Austria. http://www.R-project.org/.

Riddle, B. R., et al. 2008. The role of molecular genetics in sculpting the future of integrative biogeography. Progress in Physical Geography 32:173–202.

Ronquist, F., et al. 2012. MrBayes 3.2: efficient Bayesian phylogenetic inference and model choice across a large model space. Systematic Biology 61:539–542.

Salicini, I., C. Ibáñez, and J. Juste. 2011. Multilocus phylogeny and species delimitation within the Natterer's bat species complex in the western Palearctic. Molecular Phylogenetics and Evolution 61:888–898.

Sikes, R. S., W. L. Gannon, and the Animal Care and Use Committee of the American Society of Mammalogists. 2011. Guidelines of the American Society of Mammalogists for the use of wild mammals in research. Journal of Mammalogy 92:235–253.

Smith, S. A., P. R. Stephens, and J. J. Wiens. 2005. Replicate patterns of species richness, historical biogeography, and phylogeny in Holarctic treefrogs. Evolution 59:2433–2450.

Stanley, W. T., and R. Hutterer. 2007. Differences in abundance and species richness between shrews and rodents along an elevational gradient in the Udzungwa Mountains, Tanzania. Acta Theriologica 52:261–275.

Stanley, W. T., P. M. Kihaule, K. M. Howell, and R. Hutterer. 1998. Small mammals of the Eastern Arc Mountains, Tanzania. Journal of East African Natural History 87:91–100.

StatSoft Inc. 2011. STATISTICA v10. http://www.statsoft.com/.

Stephens, M., N. J. Smith, and P. Donnelly. 2001. A new statistical method for haplotype reconstruction from population data. American Journal of Human Genetics 68:978–989.

Tamura, K., J. Dudley, M. Nei, and S. Kumar. 2007. MEGA4: Molecular Evolutionary Genetics Analysis (MEGA) software version 4.0. Molecular Biology and Evolution 24:1596–1599.

Taylor, P. J., et al. 2009. Speciation mirrors geomorphology and palaeoclimatic history in African laminate-toothed rats (Muridae: Otomyini) of the *Otomys denti* and *Otomys lacustris* species-complexes in the "Montane Circle" of East Africa. Biological Journal of the Linnean Society 96:913–941.

Thomas, O. 1926. The generic position of certain African Muridae, hitherto referred to *Aethomys* and *Praomys*. Annals and Magazine of Natural History, Series 9, 17:174–179.

Yang, Z., and B. Rannala. 2010. Bayesian species delimitation using multilocus sequence data. Proceedings of the National Academy of Sciences of the United States of America 107:9264–9269.

Submitted 22 October 2013. Accepted 24 October 2013. Published Online 30 December 2013.

Associate Editor was Ryan W. Norris.

Appendix I

Specimens ($n = 194$) examined in this study. Specimens included in the morphometric analyses only are in standard type, those included in both the morphometric and molecular

analyses are in boldface type, and those included in the molecular analyses only are indicated with an asterisk (*). FMNH = Field Museum of Natural History; BMNH = Natural History Museum, London.

Hylomyscus kerbispeterhansi, new species (n = 68).—KENYA: Cherangani Hills, 2,740 m, 0.99973°N, 35.49372°E (FMNH 217377, 217380*, **217381**, **217382**, 217383*, **217384**, 217385*, 217386, 217387, 217388*, 217390, 217394, 217395, 217402, 217408, 217422, 217605, **217606**, **217607**, 217608–217610, 217612–217614); Mau Escarpment, 2,320 m, 0.294120°S, 35.449070°E (FMNH **210061**–**210065**, **210069**–**210071**); Mau Escarpment, 2,350 m, 0.641700°S, 35.491040°E (FMNH 209994*, **209995**, **209997**, 209999*, **210000**, **210001**, **210003**, **210015**, **210017**, **210018**, **210023**, **210038**, **210040**, 210041*, **210042**, 210043*); Mt. Elgon, 2,530 m, 1.07718°N, 34.72471°E (FMNH 217325*, 217327, 217328, **217329**–**217331**, 217333, 217340–217342, 217345, 217354, **217358**, 217597, 217598, **217599**, 217600, **217601**, 217602, 217604).

Hylomyscus anselli (n = 24).—TANZANIA: Mbizi Mts., 2,200 m, 7.8639°S, 31.6694°E (FMNH 171352*, **171353**, **171360**, 171361, **171362**, **171363**–171367); Mbizi Mts., 2,300 m, 7.8750°S, 31.6667°E (FMNH 171343, 171344, 171346–171348, 171350, 171351, 171354–171356, 171512, 171513). ZAMBIA: Mpika District, Luitikila Stream, 11°36′S, 31°34′E (BMNH 73.142); Mwinilunga District, Sakeji Stream (BMNH 61.944); Solunezi District, Nyansule Stream (BMNH 74.251).

Hylomyscus arcimontensis (n = 37).—TANZANIA: South Pare Mts., 1,100 m, 4.33°S, 38.00°E (FMNH 151253); South Pare Mts., 2,000 m, 4.28°S, 37.9278°E (FMNH 153946–153950, 153952); East Usambara Mts., 870 m, 5.10°S, 38.60°E (FMNH 150120–150125, 150142, 150143*, 150144, 150146–150150, 150153, 150430); East Usambara Mts., 1,100 m, 5.07°S, 38.62°E (FMNH 147290, 147291, 147476*); East Usambara Mts., 1,100 m, 5.07°S, 38.60°E (FMNH **150118**, **150119**, 150139); West Usambara Mts., 1,300 m, 5.07°S, 38.42°E (FMNH 150126, 150135–150138, 150154–150156, 150159).

Hylomyscus denniae (n = 4).—UGANDA: Ruwenzori Mts., 1,890 m, 0.35°N, 30.0°E (FMNH 144457*); Ruwenzori Mts., 2,667 m, 0.3666°N, 29.9833°E (FMNH 144527*); Ruwenzori Mts., 3,368 m, 0.3833°N, 29.9333°E (FMNH 144588*, 144605*).

Hylomyscus endorobae (n = 46).—KENYA: Aberdare Mts., 2,700 m, 0.239433°S, 36.708683°E (FMNH 190409, 190410, **190411**–**190413**, 190418, 190435, 190443, 190446, 190451, 190452*, 190454, 190461, **190463**, 190465, 190467, **190648**); Aberdare Mts., 3,100 m, 0.383283°S, 36.706550°E (FMNH 190468*, 190470*, **190471**, 190472, 190649, **190650**); Mau Escarpment, 2,350 m, 0.641700°S, 35.491040°E (FMNH **209989**, **209991**–**209993**, **209996**, **210048**); Mt. Kenya, 2,410 m, 0.20677°S, 37.49867°E (FMNH 217273, 217275, 217285, 217291, 217293, 217298, 217303, 217307, **217308**, **217309**, 217311, 217312, 217314, 217323); Mt. Kenya, 2,980 m, 0.16263°S, 37.44621°E (FMNH 212274, **217278**, **217279**).

Hylomyscus vulcanorum (n = 10).—BURUNDI: Rugege Highlands, Kibira National Park, 2,000 m, 3.247711°S, 29.539248°E (FMNH 137663*, 137668*). DEMOCRATIC REPUBLIC OF CONGO: Itombwe Mts., 2,090 m, 3.337351°S, 28.754433°E (FMNH 203881*, 203882*); Itombwe Mts., 2,900 m, 3.368783°S, 29.014083°E (FMNH 203907*); Kahuzi-Biega National Park, 2,195 m, 2.3000°S, 28.7000°E (FMNH 189461*, 189462*, 189466*). RWANDA: Rugege Highlands, Nyungwe National Park, 2,781 m, 2.4521°S, 29.2489°E (FMNH 207992*). UGANDA: Kigezi Highlands, Bwindi-Impenetrable National Park, 2,350 m, 1.3653°S, 29.65736°E (FMNH 157903*).

Hylomyscus stella (n = 4).—RWANDA: Rugege Highlands, Nyungwe National Park, 1,743 m, 2.5760°S, 29.2005°E (FMNH 207543*); Rugege Highlands, Nyungwe National Park, 2,120 m, 2.5015°S, 29.2376°E (FMNH 207791*). ZAIRE: Kabobo Forest, 1,250 m, 5.479000°S, 29.273000°E (FMNH 195109*, 195189*).

Hylomyscus aeta (n = 1).—RWANDA: Rugege Highlands, Nyungwe National Park, 1,782 m, 2.58069°S, 29.20242°E (FMNH 207532*).

Journal of Mammalogy, 95(1):E16, 2014

ERRATUM

Several errors appeared in the article "Integrated taxonomy within the *Hylomyscus denniae* complex (Rodentia: Muridae) and a new species from Kenya" by Demos et al., Journal of Mammalogy 95:E1-E15. The legends for Figure 3 and Figure 5 did not accurately describe the corresponding figures. The authors sincerely regret the oversight. Corrected legends for these figures are as follows:

CORRECTED FIG. 3 LEGEND

Fig. 3.—Dorsal, ventral, and lateral views of crania of *Hylomyscus*: A) *H. kerbispeterhansi,* new species (FMNH 210017 [holotype]; ONL = 26.7 mm), a female from Mau Escarpment, Kenya; B) *H. anselli* (FMNH 171362; ONL = 27.6 mm), a female from Mbizi Mountains, Tanzania; and C) *H. arcimontensis* (FMNH 150139; ONL = 24.9 mm), a male from East Usambara Mountains, Tanzania.

CORRECTED FIG. 5 LEGEND

Fig. 5.—Scatter plot of canonical variates (CV) axes 1 and 2 depicting results of discriminant function analysis performed on 14 log-transformed craniodental measurements. Projection of individual scores from 165 specimens assigned to 4 *Hylomyscus* taxa are depicted by the following symbols: ○ = *kerbispeterhansi,* + = *anselli,* □ = *arcimontensis,* ◇ = *endorobae*. Ellipses indicate 95% confidence limits for taxa.